Biosensors and Bioelectronics 49 (2013) 139–145

Contents lists available at SciVerse ScienceDirect

Biosensors and Bioelectronics

journal homepage: www.elsevier.com/locate/bios

A novel probe density controllable electrochemiluminescence biosensor for ultra-sensitive detection of Hg^{2+} based on DNA hybridization optimization with gold nanoparticles array patterned self-assembly platform

Wenhua Gao [a,b,*], An Zhang [a], Yunsheng Chen [a], Zixuan Chen [a], Yaowen Chen [b], Fushen Lu [a], Zhanguang Chen [a]

[a] Department of Chemistry, Shantou University, Shantou, Guangdong 515063, China
[b] Analysis & Testing Center, Shantou University, Shantou, Guangdong 515063, China

ARTICLE INFO

Article history:
Received 8 April 2013
Accepted 7 May 2013
Available online 15 May 2013

Keywords:
Nanoparticles array
Solid-state electrochemiluminescence
Biosensing switch
Ferrocene quench
Mercury
Structure-switching DNA

ABSTRACT

Biosensor based on DNA hybridization holds great potential to get higher sensitivity as the optimal DNA hybridization efficiency can be achieved by controlling the distribution and orientation of probe strands on the transducer surface. In this work, an innovative strategy is reported to tap the sensitivity potential of current electrochemiluminescence (ECL) biosensing system by dispersedly anchoring the DNA beacons on the gold nanoparticles (GNPs) array which was electrodeposited on the glassy carbon electrode surface, rather than simply sprawling the coil-like strands onto planar gold surface. The strategy was developed by designing a "signal-on" ECL biosensing switch fabricated on the GNPs nanopatterned electrode surface for enhanced ultra-sensitivity detection of Hg^{2+}. A 57-mer hairpin-DNA labeled with ferrocene as ECL quencher and a 13-mer DNA labeled with $Ru(bpy)_3^{2+}$ as reporter were hybridized to construct the signal generator in off-state. A 31-mer thymine (T)-rich capture-DNA was introduced to form T–T mismatches with the loop sequence of the hairpin-DNA in the presence of Hg^{2+} and induce the stem-loop open, meanwhile the ECL "signal-on" was triggered. The peak sensitivity with the lowest detection limit of 0.1 nM was achieved with the optimal GNPs number density while exorbitant GNPs deposition resulted in sensitivity deterioration for the biosensor. We expect the present strategy could lead the renovation of the existing probe-immobilized ECL genosensor design to get an even higher sensitivity in ultralow level of target detection such as the identification of genetic diseases and disorders in basic research and clinical application.

1. Introduction

DNA, with its perfect specificity for bioactive molecules, has been widely used to construct the biosensor to assay DNA samples and provide escalating quantities of proteins information (Campas and Katakis, 2004; Turner, 2000). Recent years have witnessed the development of various DNA biosensors based on different detection methods including optical (Ahn and Walt, 2005; Parab et al., 2010), electrochemical (Li et al., 2012; Park et al., 2002), electrochemiluminescence (ECL) (Sun et al., 2010; Yao et al., 2009), quartz-crystal microbalance (Su et al., 2004; Yamaguchi and Shimomura, 1993), and surface plasmon resonance (SPR) techniques (Ito et al., 2007; Law et al., 2011). As an alternative, biosensor based on ECL hold great promise since it could combine the advantages of both electrochemical and chemiluminescent, such as strong signal response, inherent sensitivity, simplified optical setup and low background signal.

In medicine and molecular diagnostics, it is always a great challenge for the detection and quantification of extremely low concentrations of target molecules such as ultralow level genetic disorders and protein biomarkers in the early stage of diseases. Considerable effort has been made to develop novel ECL biosensor with high sensitivity. It includes, on the one hand, improving efficiency of signal production unit such as development of new high quantum efficiency ECL labels (Bruno and Kiel, 2002; Calvo-Munoz et al., 2005; Fang et al., 2008; Huang et al., 2009), exploration of multilabeling approach (Li et al., 2007; Miao and Bard, 2004; Wang et al., 2006) and application of nanomaterial as label carrier (Chang et al., 2006; Y. Li et al., 2010; Zhu et al., 2008)

* Corresponding author at: Shantou University, Department of Chemistry, 243 Daxue Road, Shantou, Guangdong 515063, China. Tel.: +86 754 82902774; fax: +86 754 82903941.
E-mail address: whgao@stu.edu.cn (W. Gao).

0956-5663/$ - see front matter © 2013 Elsevier B.V. All rights reserved.
http://dx.doi.org/10.1016/j.bios.2013.05.013

to offer a remarkable amplification of DNA hybridization events; on the other hand, optimizing the structure of target identification unit such as use of DNA hairpins as molecular beacons for label-free detection of oligonucleotide (Broude, 2002; Zhang et al., 2008), application of modular allosteric aptamer sensor design (Bang et al., 2013; Y. Li et al., 2008), stem-loop fluorescence molecular beacons (Du et al., 2005; Jin et al., 2006; Tyagi and Kramer, 1996), adoption of rolling circle amplification-electrochemiluminescence sensor (Zhou et al., 2012) and fabrication of solid-state ECL (Wang et al., 2009; Zhu et al., 2009, 2010). However, as the substrate of biosensor fabrication, the self-assembly platform itself has received far less attention. Thus, work on investigating whether the substrate itself could serve as an efficient sensitivity-enhancement agent is set to our schedule.

Intuitively, one would imagine that an ever-increasing density of surface bound probes would lead to an increasingly better sensor performance since more probes mean more beacons and higher signal response. However, as the DNA probes are immobilized, we must take note of the fact that superfluous DNA flexible chain could bring greater steric which really affects the hybridization efficiency between the probe and target sequence (Berganza et al., 2007; Henry et al., 1999; Peterson et al., 2001; Tokuhisa et al., 2009; Yguerabide and Ceballos, 1995). Recently, Soreta et al. (2011) have reported a promising approach to fabricate electrochemical DNA biosensors on gold nanoparticles (GNPs) patterned glassy carbon electrode (GCE) by concentrating their efforts on the optimization of the DNA probe density and achieved high sensitivity for the electrochemical biosensor, whereas one problem was also put forward that the response signal generated may be too low to be of any analytical value as the number of DNA molecule beacon is limited by the GNPs anchor point number. Fortunately, the problem could be solved when it comes to ECL biosensing system. Unlike electrochemical signal detection method, based on the inherent strong luminescence feature of each individual ECL reporter, the weak luminescence signal can be still detected even if the density of molecule beacon and target DNA is very low.

Thus, a new way is opened up to further promote the sensitivity of ECL biosensing system through controlling the probe density on the electrode surface. Along the promising way, the present work for the first time applied the number density controlled GNPs array as self-assembly platform for ECL biosensor fabrication and successfully built up a sensitivity-enhanced ECL biosensor for Hg^{2+}. The design of the structure-switching ECL biosensor is shown in Scheme 1. For the sensor, a thiolated 57-mer hairpin DNA (h-DNA) and a 31-mer thymine-rich (T-rich) capture DNA (c-DNA) were designed to capture Hg^{2+} in the light of the theory that Hg^{2+} could specifically bind two DNA thymine (T) bases and promote the T–T mismatch forming stable base pairs (Ono and Togashi, 2004; Tanaka et al., 2007). Since ferrocene (Fc) could perform an efficient and stable quenching effect on ECL of tris(2,2′-bipyridine)ruthenium(II) [$Ru(bpy)_3^{2+}$] and the quenching effect is related to the distance between reporter and quencher molecule (Cao et al., 2006; X. Wang et al., 2008), Ru $(bpy)_3^{2+}$ as luminescence reporter and Fc as luminescence quencher were used to mark the h-DNA and the 13-mer signal DNA (s-DNA), respectively. The 13-mer s-DNA with the $Ru(bpy)_3^{2+}$ tag at 5′-end was attached to h-DNA by five base pairs hybridization and the ECL can be kept in quenching by the Fc label on the 3′-end of h-DNA in folded configuration. The h-DNA was linked to the GNPs by the mercapto group at 5′-terminal and its "hairpin-linear" switchable structure determined the "signal off–on" switch feature of the ECL biosensor. As that there are only 9 base pairs between c-DNA and h-DNA, the hairpin DNA could maintain folded configuration before binding Hg^{2+}. In the presence of Hg^{2+}, the T-rich c-DNA could hybridize with the loop sequence of h-DNA to induce the h-DNA stem-loop convert from folded configuration into a linear double helix, coincided with the transformation of luminescence signal from "off" to "on". The mercaptohexanol (MCH) short strands were also introduced to backfill the uncovered GNPs surface and keep the probe strands standing up. At last, with a lower limit of detection (LOD) and enhanced ultra-high sensitivity, the "signal-on" ECL biosensor was successfully applied for ultrasensitive detection of Hg^{2+} which is a kind of highly toxic heavy metal ion and well known as hazardous pollutant with recognized accumulative character in the environment and biota (Eisler, 2003; Wang et al., 2004).

2. Experimental

2.1. Reagents and apparatus

Oligonucleotides were purchased from Sangon Bioengineering Ltd. Company (Shanghai, China) and their sequences are shown as follows. (bolded bases are self-complementary stem segments of h-DNA and italic sequence are intrinsically complimentary segments)

h-DNA: 5′–SH-$(CH_2)_6$-*GGTTGGTGTGGTT*G**GTGAGC**CTTCTTTTCTT-TTTCGCTTTTCTTTTCTTTC**GCTCAC**-$(CH_2)_6$-NH_2-3′

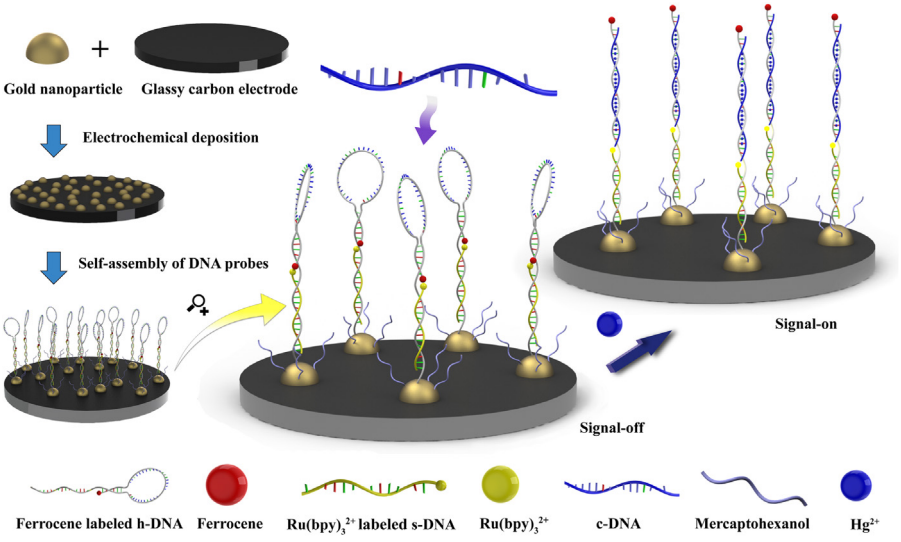

Scheme 1. Schematic illustration of the design and preparation of the ECL biosensor for Hg^{2+} detection .

s-DNA: 3′–*CCAACCACACCAA*-$(CH_2)_6$-NH_2-5′
c-DNA: 3′–GTTGTTTTGTTTTTGCGTTTTGTTTTGTTTG-5′
Auxiliary-DNA: 3′–CAAGAAAAGAAAAAGCGAAAAGAAAAGAAAG-5′

Tripropylamine (TPrA), 2,2′-bipyridine (bpy), N-hydroxysuccinimide ester (NHS), ferrocene acetic acid (FcA) and Tetrachloroauric(III) acid tetrahydrate [$HAuCl_4 \cdot 4H_2O$] were obtained from Aladdin Chemical Reagent Co. Ltd. (Shanghai, China). MCH, sodium-perchlorate [$NaClO_4$], mercury nitrate [$Hg(NO_3)_2$] and other metal salts were purchased from Sigma-Aldrich (St. Louis, MO, USA). Ruthenium (III) chloride hydrate, 2,2′-bipyridyl-4,4′-dicarboxylic acid (dcbpy), sodium hexafluorophosphate, N-(3-dimethylaminopropyl)-N′-ethyl-carbodiimide (EDC), N,N′-dicyclohexyl carbodiimide (DCC) were purchased from Sinopharm Chemical Reagent Co. Ltd. (Shanghai, China). All other chemicals not mentioned here were of analytical reagent grade and were used as received. Millipore Milli-Q water (18 ΩM cm) supplied by a Millipore Milli-Q water purification system (Bedford, MA. USA) was used throughout. A concentration of 0.10 M phosphate buffer saline (PBS, pH 7.5, 0.10 M NaCl+0.10 M NaH_2PO_4/Na_2HPO_4) was used as hybridization buffer, binding buffer and washing solution.

A traditional three-electrode system composed of a bare GCE (3 mm in diameter) or biosensor as working electrode, a platinum wire as counter electrode and a Ag/AgCl (1 M KCl) as reference electrode was applied in a 10 mL glass analytical cell. ECL curve was recorded on a computerized MPI-B type ultra-weak luminescence analyzer (Xi'an Remax Electronic Science Tech. Co. Ltd., China) equipped with a photomultiplier allowing maximum operating voltage of −1000 V. An IM6e electrochemical workstation (Zahner IM6e, Germany) was used to carry out impedance measurement. The UV–vis spectrum was recorded on a Lambda 950 spectrophotometer (Perkin Elmer, USA). Scanning electron microscopy for characterization of the electrochemically nucleated GNPs array on a commercial detachable GCE (3 mm in diameter, Gaoss Union Instrument Inc., China) was carried out using a JSM-6360LA (JEOL, Japan). Sample analysis was performed with Agilent 7500 inductively coupled plasma-mass spectrometry (ICP-MS, Agilent, USA).

2.2. Electrode cleaning, conditioning, and electrochemical deposition of GNPs

GCE was polished with 0.3 and 0.05 μm α-Al_2O_3 slurry and then washed ultrasonically with 50% (V/V) ethanol–water solution twice and pure water once successively, followed by electrochemical conditioning by potential scanning from 0 to 1.4 V in 1 M $NaClO_4$ for at least five complete scans at 50 mV s^{-1} until a reproducible cyclic voltammogram was obtained. Then the electrode was immediately used for deposition modification after a rinse step.

The deposition of GNPs with different number density was performed by immersing the polished electrode into gradient concentrations (40, 70, 100, and 140 μM) of $HAuCl_4$ solution in 5 mL of 0.5 M potassium nitrate and applying a 5 s potential step from 1.1 to −1.0 V. For control experiments, GCE almost completely covered with gold layer were prepared by extending the deposition time to 20 s in 200 μM $HAuCl_4$ deposition solution in 0.5 M potassium nitrate.

2.3. Synthesis of ECL reporting probe and quenching probe

Ruthenium bis(2,2′-bipyridine)-(2,2′-bipyridine-4,4′-dicarboxylic acid)-N-hydroxy succinimide ester ($Ru(bpy)_2$(dcbpy)NHS) was synthesized according to previously reported method (Sprintschnik et al., 1976; Sullivan et al., 1978; Terpetschnig et al., 1995; Zhang et al., 2008) through DCC with some modification and directly used to mark the s-DNA to obtain the luminescence probe of $Ru(bpy)_2$(dcbpy)NHS-DNA (abbreviated as Ru-Pro). The Ru-Pro was characterized by UV–vis spectroscopy (Fig. S1) to verify that $Ru(bpy)_2$(dcbpy)NHS was indeed labeled on s-DNA and the concentration was estimated, on the basis of UV absorbance at 457 nm, to be 7.01×10^{-5} M (Li et al., 2010; Shimdzu et al., 1985). Ferrocene-labeled DNA (abbreviated as Fc-Pro) as quenching probe was prepared by chemically binding FcA to the terminal 5′-amino of h-DNA in the presence of a water-soluble EDC according to previous reported method (X. Wang et al., 2008). The Fc-Pro obtained was finally suspended in 10 mM PBS solution (pH 7.5), and stored at 4 °C for later use. More details of the Ru-Pro and Fc-Pro synthesis can be found in the supporting information.

2.4. Fabrication of sensor in "signal-off"

The Fc-Pro was tethered onto the GNPs with a conventional self-assembly method based on thiol-Au bonding reaction by pipetting 20 μL of ~1 μM diluted Fc-Pro solution onto the GCE surface immediately after the gold electrodeposition step allowing the thiol-Au interaction to sustain for at least 3 h meanwhile the solvent should be kept unexhausted. Then the Fc-Pro modified GCE (Fc-Pro-GCE) was thoroughly washed in a stirred solution of PBS for 20 min to remove any weakly bound Fc-Pro and non-specific adsorption was minimized. In order to obtain well-aligned DNA monolayers, the modified electrode was then treated with 1 mM MCH solution in PBS for 30 min at room temperature and washed again. Thus the uncovered gold nanoparticle surface was backfilled with MCH strands and the h-DNA strands can be kept standing up rather than lying down on the sensor surface. Finally, through complementary sequence hybridization of h-DNA to s-DNA and c-DNA, Ru-Pro and c-DNA was introduced to the h-DNA by sequentially immersing the Fc-Pro-GCE in 500 μL of ~7 μM Ru-Pro solution for 2 h and 500 μL of 10 μM c-DNA solution for 1 h at 37 °C, followed by a rinse process as above.

2.5. ECL measurement of Hg^{2+}

Various concentrations of Hg^{2+} (500, 250, 100 , 50, 10, 5, 1, and 0.1 nM) were prepared for determining the sensitivity and LOD of the biosensor by serial dilution of the $Hg(NO_3)_2$ stock solution. After a pre-scan to record the luminescence intensity of the "signal-off" sensor, the sensor was immersed in 100 μL PBS containing certain concentration of Hg^{2+} for a period of time at 25 °C followed by a 5 min rinse in PBS to remove any unbound substances. Then, the ECL determinations were performed at room temperature in 20 mM PBS containing 0.1 M TPrA (pH 7.5). The cyclic voltammetry (CV) mode with continuous potential scanning from 0.2 to 1.2 V at a scanning rate of 0.1 V s^{-1} was adopted. The supersaturated TPrA solution was prepared as previous protocol (S.J. Wang et al., 2008). A high voltage of −800 V was supplied to the photomultiplier for luminescence intensity determination.

3. Results and discussion

3.1. Characterization of the biosensing electrode impedance

Electrochemical impedance spectroscopy (EIS) was adopted to monitor the fabrication processes of the biosensing electrode and characterize the impedance feature of nanopatterned GCE with different number density of GNPs. In the form of Nyquist plot, Fig. 1 shows the impedance spectra obtained in the investigation. As Fig. 1A shows, the bare GCE gave an almost linear arc plot with a micro radian in high frequency region and behaved as an ideal conductor, indicating a very fast electron transfer process of $[Fe(CN)_6]^{3-/4-}$ (curve a, Fig. 1A). Inset of Fig. 1A shows the equivalent circuit used to fit the data, the components in the

equivalent circuit included the solution resistance R_s, charge-transfer resistance R_{ct}, constant phase element (CPE) related to double layer capacitance, Warburg impedance Z_w, where $Z_w = R_w/(j_w)^{1/2}$ and R_w is the diffusion resistance (Patolsky et al., 2001). The R_{ct} of bare GCE can be estimated to be 3.038 kΩ and then increased to 9.586 kΩ (curve b, Fig. 1A) for the GNPs array modified electrode since the inhomogeneous electrode surfaces caused by GNPs could affect the impedance feature of the system (Juttner, 1990). Interestingly, self-assembly of the thiolated Fc-DNA seemed as if benefit to recover the electro-conductibility of the GNPs–GCE with an obvious electrochemical impedance decrease (curve c, Fig. 1A) and the R_{ct} dropped to 3.176 kΩ, which appeared to be not in line with the previously reported result that Fc-DNA could lead to increased electrochemical impedance (Wang et al., 2009). It is also obvious that conformational transition induced by Hg^{2+} could produce negative impedance performance (8.544 kΩ, curve d, Fig. 1A) since the facilitate effect of Fc could fade with the increased distance.

For this distinctive result, we give out our presumption as follows. Hypothetically, rather than the Fc-DNA, it is precisely the Fc with a C_5H_5–iron–C_5H_5 sandwiched electron-rich structure improved the electron transfer of GNPs–GCE while the DNA strands could conversely hinder electron transfer. As the probe distribution is controllable, the Fc label at the terminal of folding hairpin-shaped DNA is confined to the electrode surface in a negligible distance and could facilitate electron transfer to the best itself, meanwhile the negative role of DNA was covered up due to its sparse distribution. However, as the DNA distribution is not controllable and in high number density, the DNA layer could act as a shielding layer between the electrode surface and outside solution and results in low electron transfer efficiency of the system. To verify the presumption, the sensors fabricated with probe of different number density were also performed EIS

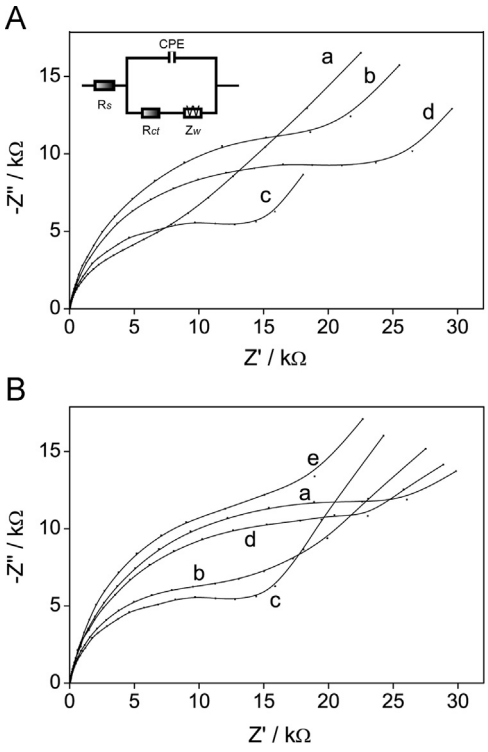

Fig. 1. A: Nyquist plot for electrochemical impedance measurements in 5.0 mM $[Fe(CN)_6]^{3-/4-}$ solution for the bare GCE (a), gold nanoparticles array modified GCE (b), DNA probe self-assembly monolayer modified GCE biosensor (c), and GCE biosensor after binding with Hg^{2+} (d). Inset is the equivalent circuit used to fit the data. B: Impedance measurement plots for DNA modified GCE after electrochemical deposition with $HAuCl_4$ solution of 40 (a), 70 (b), 100 (c), 140 (d) and 200 μM (e).

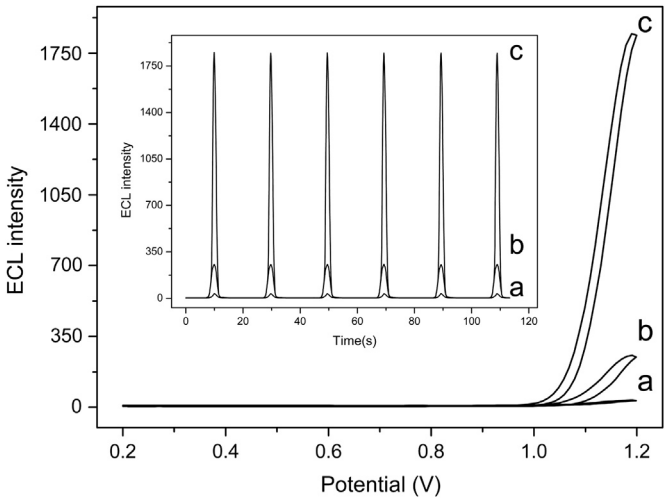

Fig. 2. ECL intensity *vs.* potential curves for the bare GNPs-GCE without any DNA probe (a), the GNPs-GCE biosensor modified with Ru-Pro and Fc-Pro (b), and the biosensor after hybridization with the a-DNA (c). Inset: ECL intensity *vs.* time curves for the biosensor under continuous CV for six cycles. ECL curves were measured in 20 mM PBS containing 1.0 mM TPrA at 0.1 V s^{-1}.

characterization and the result is shown in Fig. 1B. There really exists an optimum probe density for the sensor impedance feature as the deposition solution adopted reached 100 μM (curve a, b and c, Fig. 1B) and even higher probe density really deteriorated the impedance performance (curve d and e, Fig. 1B). Thus it can be found that controllable DNA distribution could also avoid the electrode conductance deterioration caused by DNA strands and get the biosensor electrode a perfect electron transport performance which is also conducive to improve the signal response property of the sensor.

3.2. Stability of the GNPs array as self-assembly platform

To explore the stability of the GNPs array as self-assembly platform and its latent practicability in DNA hybridization ECL biosensing, the 37-mer auxiliary-DNA (a-DNA) strand intrinsically complementary to the T-rich fragment of h-DNA was introduced to get a linear double helix. The corresponding ECL intensity-potential curves of the biosensing electrode are presented in Fig. 2. As the Fig. 2 shows, there is no obvious ECL signal response can be found for the bare GNPs-GCE (curve a), while the fabrication of Fc-Pro and Ru-Pro onto GNPs resulted in a weak ECL signal response (curve b). After the hybridization with a-DNA, a striking increase of ECL signal was found as the Fc groups got away from the $Ru(bpy)_3^{2+}$ group and "signal-on" status was achieved (curve c). Moreover, as shown in the inset of Fig. 2, continuous CV scanning the electrode can give an balanced ECL intensity which indicate that the Ru-Pro can be stably attached to the GNPs array self-assembly platform via Au–S interactions without $Ru(bpy)_3^{2+}$ escape from the electrode surface.

3.3. Effect of probe number density on the detection of Hg^{2+}

Focusing effect on optimizing the DNA probe number density, the relationship between GNPs number density and biosensor sensitivity was investigated to find an optimal condition for the detection of Hg^{2+}. The performance of ECL biosensors with different density of GNPs was assessed by quantitative determination of Hg^{2+} in the concentration range of 1–500 nM. As shown in Fig. 3, one optimal sensitivity defined as calibration curve slope was achieved for the sensor in condition c (calibration curve

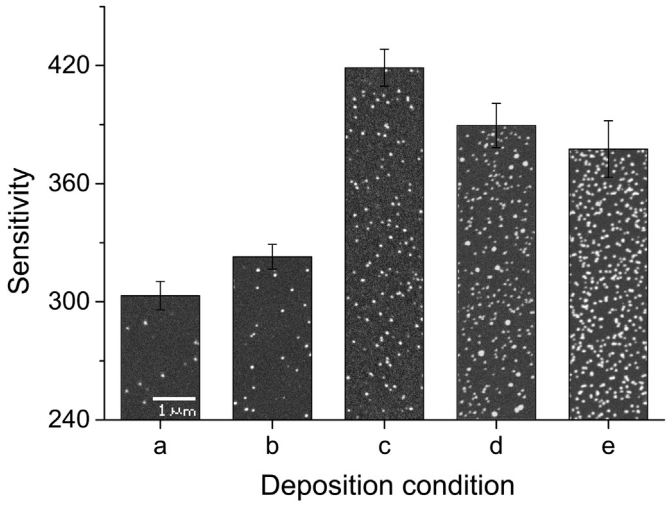

Fig. 3. Performance comparison of the biosensors fabricated in different $HAuCl_4$ deposition condition of 40 (a), 70 (b), 100 (c), 140 μM (d) applying a 5 s potential step and 200 μM (e) applying a 30 s potential step from 1.1 to −1.0 V. The fill pattern for each column present the SEM image of GNPs array corresponding to above deposition condition. Sensitivity is defined as the slope of the sensor calibration curves for the detection of Hg^{2+} in the range 1–500 nM (error bar is based on 3 times assay for each specific concentration).

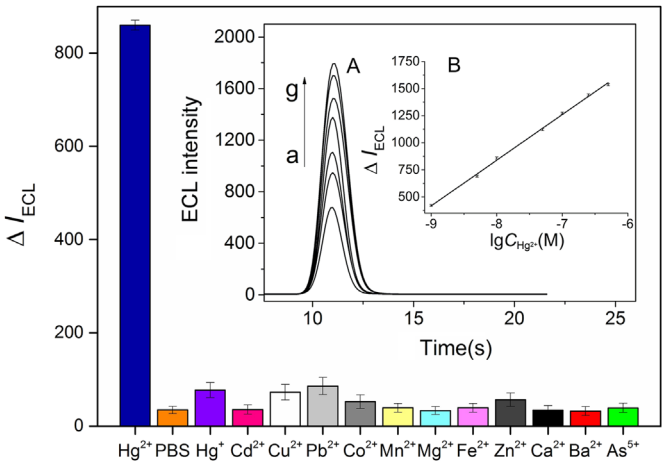

Fig. 4. Effects of various metal ions on the ECL signal response measured by the optimal ECL biosensor. The concentration of Hg^{2+} used was 10 nM, whereas the concentration of the other tested metal ions was 500 nM. Error bars represent the standard deviation of three repetitive experiments. Inset: (A) ECL intensity-time curves for the biosensor with optimal probe number density after binding with various concentration of Hg^{2+}. The concentrations of Hg^{2+} were 1 (a), 5 (b), 10 (c), 50 (d), 100 (e), 250 (f) and 500 nM (g), respectively. (B) The calibration curve of the ECL response as a function of the concentration of Hg^{2+}. Error bars represent the standard deviation of five parallel experiments.

corresponding to each condition can be found in Fig. S2), and while further more GNPs and signal probes result in deterioration of the sensor performance. This abnormal but interesting result may be explained as follows. In general, stronger response signal means higher sensitivity for a biosensor and it is necessary to equip the biosensor with sufficient signal probe to produce instrument detectable signal. However, more probe strands in certain area means higher steric hindrance which could greatly deteriorate the hybridization efficiency between probe strands and target DNA strands and thus weaken the response signal. It is not hard to envisage that once the trace Hg^{2+} ions capable of inducing conformational transition of just one hundred h-DNA were carved up by sheer amount of such probes, the limited T–Hg^{2+}–T bind sites for each probe strand may fail to uncurl the loop strand into linear double helix and the weak response signal was drowned by noisy signal. Moreover, as the sensitivity variation trend is in good accordance with the former result of electrode impedance, we concluded that the worse conductivity of the electrode due to more DNA shield also plays a role in corrupting the sensor sensitivity.

3.4. Incubation time of ECL biosensing electrode with Hg^{2+}

The effect of the incubation time on the sensor performance at Hg^{2+} concentration of 1, 10, 500 nM were also investigated and shown in Fig. S3. As the incubation time increased, the ECL intensity change (ΔI_{ECL}) increased rapidly and reached a plateau after 20 min suggesting that the T–Hg^{2+}–T stands was forming gradually and an almost complete binding reached. This binding time for T–Hg^{2+}–T interaction is shorter than previously reported result of 30 min (Finot et al., 1999). For this result, we can concluded that well-aligned DNA like forest rather than shrubbery growing on the well-distributed GNPs array could more easily capture the free Hg^{2+} in solution without large steric effect. Moreover, the lower number density of probe is also conducive to make all the strands reach binding equilibrium in a shorter period.

3.5. Sensitivity and selectivity

With the optimized probe density, the sensitivity of ECL biosensor was assessed by measuring the dependence of ΔI_{ECL} upon the concentration of Hg^{2+}. As the inset A of Fig. 4 shows, the ECL intensity was enhanced as higher concentration of Hg^{2+} was used for binding the probes, and the ΔI_{ECL} was found to be logarithmically related to the concentration of Hg^{2+} in the range from 1 to 100 nM (inset B of Fig. 4). The regression equation is $\Delta I_{ECL}=421\ lgC_{Hg}{}^{2+}+4209$ with a regression coefficient of 0.9985 and detection limit of 0.1 nM. This LOD, which is defined as the concentration corresponding to the mean blank value plus 3 standard deviations, is 2 orders of magnitude lower than the Maximum Contaminant Level in drinking water set forth by the United States Environmental Protection Agency (USEPA) in the Clean Water Act of 2 ppb (10 nM). Moreover, this approach provides an method to get the Hg^{2+} biosensor a ultrahigh sensitivity with an LOD about 1–2 orders of magnitude lower than other reported works for Hg^{2+} detection such as the ECL biosensor fabricated on planar gold electrode (Zhu et al., 2010), ECL biosensor fabricated with magnetic beads (Q. Li et al., 2010), fluorescence probe biosensor (Tian et al., 2010), electrochemistry biosensor (Zhuang et al., 2013) and the SPR biosensing method (Chang et al., 2011), but in same level of the rolling circle amplification method of Zhou et al. (2012). One detailed comparison of the proposed biosensor can be found in Table S1 in the supporting information. Thus, it can be concluded that the ECL biosensor developed here by anchoring hairpin DNA probes on number density controllable nanoparticle array could really realize ultrasensitive detection of Hg^{2+}. The Hg^{2+} biosensor based on this system hold great promise in environmental monitoring of the exposure of Hg^{2+}.

To assess the selectivity of the T-rich probe to other interferent ions, various ions possibly coexisting with Hg^{2+} was individually examined at 25 °C for 1 h. As shown in Fig. 4, the sensor showed significant ECL increase in response to Hg^{2+}, but hardly exhibited substantial responses to other metal ions with concentration of 500 nM which is 50 times that of Hg^{2+}. Note that the biosensor presented very low ECL response (~10% of the Hg^{2+} effect) to Hg^{+}, Cu^{2+} and Pb^{2+}, which could possibly exhibit weak coordination with T (D. Li et al., 2008; Liu et al., 2009), the interference from the possible competing ions was merely eliminated in the present work. This can be attributed to the fact that the weak coordination with T can hardly cause stable conformational transition of the T-rich probe. Therefore, it can be concluded that this biosensor presented a satisfactory selectivity for Hg^{2+}.

Table 1
Determination the concentrations of Hg^{2+} in water samples using the proposed method and ICP-MS [a].

Sample	Biosensing method (nM)	ICP-MS method (nM)	Relative deviation (%)
Outfall 1	75.32 ± 3.16	74.51 ± 3.08	1.09
Outfall 2	86.42 ± 6.18	85.31 ± 5.97	1.30
Outfall 3	91.82 ± 8.27	92.36 ± 7.78	−0.58
Outfall 4	102.88 ± 8.69	103.77 ± 9.12	−0.86

[a] All values were obtained as average of three repetitive determinations plus standard deviation.

3.6. Direct detection of Hg^{2+} in water samples

The applications of the biosensor based on the GNPs array were evaluated for determination of Hg^{2+} in natural water. The concentration of Hg^{2+} was determined by the biosensing method as well as ICP-MS. The river water sample was collected at four sewage outfalls along the Guihua River in Shantou, China. The samples collected were filtered through 0.2 μm membranes to remove impurities and diluted with equal volume of PBS solution. As shown in Table 1, the results using our biosensor are in good agreement with those achieved using the ICP-MS method.

4. Conclusions

We have pioneered to introduce the GNPs nanostructured self-assembly platform into ECL biosensing system and successfully fabricated a "signal-on" solid-state ECL biosensor for sensitive and selective detection of Hg^{2+}. This ECL biosensor based on GNPs array platform hold several advantages. Firstly, the DNA probe distribution is well controlled by the platform and a high hybridization efficiency is secured. Secondly, the response patterns of $Ru(bpy)_3^{2+}$ to TPrA afford a strong signal response even if the probe density is very low to meet the analysis available value. Thirdly, the lower density and optimized distribution of the probe could earn the biosensor a time-saving character for rapid detection. It was demonstrated in this work that the sensitivity of DNA-based ECL biosensor could be greatly improved with lower LOD using the GNPs array modified electrode to control the spacing and orientation of immobilized DNA probe. Objectively, we should also note that the reusability needs to be get more improvement to meet the requirement of practical sample analysis. In summary, we expect the proposed DNA–GNPs array self-assemble method could do help to renovate most of the current ECL biosensor built on planar surface and get an enhanced super high sensitivity in bioanalysis.

Acknowledgments

We are grateful for the financial support from the Guangzhou Associated & Service Center of Scientific Instrument (No. 201201), Research Start-up Funding of Shantou University, the Natural Science Foundation of Guangdong Province (No. S2011010005208) and the National Natural Science Foundation of China (No. 51272152/E0208).

Appendix A. Supporting information

Supplementary data associated with this article can be found in the online version at http://dx.doi.org/10.1016/j.bios.2013.05.013.

References

Ahn, S., Walt, D.R., 2005. Analytical Chemistry 77, 5041–5047.
Bang, J.S., Cho, S., Lee, N., Lee, B.R., Kim, J.H., Kim, B.G., 2013. Biosensors and Bioelectronics 39, 44–50.
Berganza, J., Olabarria, G., Garcia, R., Verdoy, D., Rebollo, A., Arana, S., 2007. Biosensors and Bioelectronics 22, 2132–2137.
Broude, N.E., 2002. Trends Biotechnology 20, 249–256.
Bruno, J.G., Kiel, J.L., 2002. Biotechniques 32, 178–183.
Calvo-Munoz, M.L., Dupont-Filliard, A., Billon, M., Guillerez, S., Bidan, G., Marquett, C., Blum, L., 2005. Bioelectrochemistry 66, 139–143.
Campas, M., Katakis, I., 2004. Trends in Analytical Chemistry 23, 49–62.
Cao, W., Ferrance, J.P., Demas, J., Landers, J.P., 2006. Journal of the American Chemical Society 128, 7572–7578.
Chang, C.C., Lin, S., Wei, S.C., Chen, C.Y., Lin, C.W., 2011. Biosensors and Bioelectronics 30, 235–240.
Chang, Z., Zhou, J.G., Zhao, K., Zhu, N.G., He, P.G., Fang, Y.Z., 2006. Electrochimica Acta 52, 575.
Du, H., Strohsahl, C.M., Camera, J., Miller, B.L., Krauss, T.D., 2005. Journal of the American Chemical Society. 127, 7932–7940.
Eisler, R., 2003. Environmental Geochemistry and Health 25, 325–345.
Fang, L.Y., Lu, Z.Z., Wei, H., Wang, E.K., 2008. Analytica Chimica Acta 628, 80–86.
Finot, M.O., Braybrook, G.D., McDermott, M.T., 1999. Journal of Electroanalytical Chemistry 466, 234–241.
Henry, M.R., Stevens, P.W., Sun, J., Kelso, D.M., 1999. Analytical Biochemistry 276, 204–214.
Huang, H., Jie, G., Cui, R., Zhu, J.J., 2009. Electrochemistry Communications 11, 816–818.
Ito, M., Nakamura, F., Baba, A., Tamada, K., Ushijima, H., Lau, K.H.A., Manna, A., Knoll, W., 2007. Journal of Physical Chemistry C 111, 11653–11662.
Jin, Y., Yao, X., Liu, Q., Li, J.H., 2006. Biosensors and Bioelectronics 22, 1126–1130.
Juttner, K., 1990. Electrochimica Acta 35, 1501–1508.
Law, W.C., Yong, K.T., Baev, A., Prasad, P.N., 2011. ACS Nano 5, 4858–4864.
Li, D., Wieckowska, A., Willner, I., 2008. Angewandte Chemie International Edition 47, 3927–3931.
Li, Q., Zhou, X., Xing, D., 2010. Biosensors and Bioelectronics 26, 859–862.
Li, W., Wu, P., Zhang, H., Cai, C.X., 2012. Analytical Chemistry 84, 7583–7590.
Li, Y., Qi, H.L., Fang, F., Zhang, C.X., 2007. Talanta 72, 1704–1709.
Li, Y., Qi, H.L., Gao, Q., Yang, J., Zhang, C.X., 2010. Biosensors and Bioelectronics 26, 754–759.
Li, Y., Qi, H.L., Peng, Y.G., Gao, Q., Zhang, C.X., 2008. Electrochemistry Communications 10, 1322–1325.
Liu, S.J., Nie, H.G., Jiang, J.H., Shen, G.L., Yu, R.Q., 2009. Analytical Chemistry 81, 5724–5730.
Miao, W.J., Bard, A.J., 2004. Analytical Chemistry 76, 5379–5386.
Ono, A., Togashi, H., 2004. Angewandte Chemie International Edition 43, 4300–4302.
Parab, H.J., Jung, C., Lee, J.H., Park, H.G., 2010. Biosensors and Bioelectronics 26, 667–673.
Park, S.J., Taton, T.A., Mirkin, C.A., 2002. Science 295, 1503–1506.
Patolsky, F., Lichtenstein, A., Willner, I., 2001. Journal of the American Chemical Society. 123, 5194–5205.
Peterson, A.W., Heaton, R.J., Georgiadis, R.M., 2001. Nucleic Acids Research 29, 5163–5168.
Shimdzu, T., Iyoda, T., Izaki, K., 1985. Journal of Physical Chemistry 89, 642–645.
Soreta, T.R., Henry, O.Y.F., O'Sullivan, C.K., 2011. Biosensors and Bioelectronics 26, 3962–3966.
Sprintschnik, G., Sprintschnik, H.W., Kirsch, P.P., Whitten, D.G., 1976. Journal of the American Chemical Society. 98, 4947–4954.
Su, X.D., Robelek, R., Wu, Y.J., Wang, G.Y., Knoll, W., 2004. Analytical Chemistry 76, 489–494.
Sullivan, B.P., Salmon, D.J., Meyer, T.J., 1978. Inorganic Chemistry 17, 3334–3341.
Sun, B., Qi, H.L., Ma, F., Gao, Q., Zhang, C.X., Miao, W.J., 2010. Analytical Chemistry 82, 5046–5052.
Tanaka, Y., Oda, S., Yamaguchi, H., Kondo, Y., Kojima, C., Ono, A., 2007. Journal of the American Chemical Society 129, 244–245.
Terpetschnig, E., Szmacinski, H., Malak, H., Lakowicz, J.R., 1995. Biophysical Journal 68, 342–350.
Tian, M., Ihmels, H., Benner, K., 2010. Chemical Communications 46, 5719–5721.
Tokuhisa, H., Liu, J.A., Omori, K., Kanesato, M., Hiratani, K., Baker, L.A., 2009. Langmuir 25, 1633–1637.
Turner, A.P.F., 2000. Science 290, 1315–1317.
Tyagi, S., Kramer, F.R., 1996. Nature Biotechnology 14, 303–308.
Wang, H., Zhang, C.X., Li, Y., Qi, H.L., 2006. Analytica Chimica Acta 575, 205–211.
Wang, Q.R., Kim, D., Dionysiou, D.D., Sorial, G.A., Timberlake, D., 2004. Environmental Pollution 131, 323–336.
Wang, S.J., Neshkova, M.T., Miao, W.J., 2008. Electrochimica Acta 53, 7661–7667.
Wang, X.Y., Dong, P., Yun, W., Xu, Y., He, P.G., Fang, Y.Z., 2009. Biosensors and Bioelectronics 24, 3288–3292.
Wang, X., Yun, W., Dong, P., Zhou, J., He, P.G., Fang, Y.Z., 2008. Langmuir 24, 2200–2205.
Yamaguchi, S., Shimomura, T., 1993. Analytical Chemistry. 65, 1925–1927.
Yao, W., Wang, L., Wang, H.Y., Zhang, X.L., Li, L., 2009. Biosensors and Bioelectronics 24, 3269–3274.
Yguerabide, J., Ceballos, A., 1995. Analytical Biochemistry 228, 208–220.
Zhang, J., Qi, H.L., Li, Y., Yang, J., Gao, Q., Zhang, C.X., 2008. Analytical Chemistry 80, 2888–2894.

Zhou, X., Su, Q., Xing, D., 2012. Analytica Chimica Acta 713, 45–49.
Zhu, D.B., Tang, Y.B., Xing, D., Chen, W.R., 2008. Analytical Chemistry 80, 3566–3571.
Zhu, D.B., Xing, D., Tang, Y.B., Zhang, L., 2009. Biosensors and Bioelectronics 24, 3306–3310.
Zhu, X., Chen, L.F., Lin, Z.Y., Qiu, B., Chen, G.N., 2010. Chemical Communications 46, 3149–3151.
Zhuang, J., Fu, L., Tang, D., Xu, M., Chen, G., Yang, H., 2013. Biosensors and Bioelectronics 39, 315–319.